Impact of Large-Scale Circulation on Tropical Storm Frequency, Intensity, and Location, Simulated by an Ensemble of GCM Integrations

F. VITART

Program in Atmospheric and Oceanic Science, Princeton University, Princeton, New Jersey

J. L. ANDERSON AND W. F. STERN

NOAA/GFDL, Princeton University, Princeton, New Jersey

(Manuscript received 6 July 1998, in final form 25 January 1999)

ABSTRACT

Tropical storms simulated by a nine-member ensemble of GCM integrations forced by observed SSTs have been tracked by an objective procedure for the period 1980–88. Statistics on tropical storm frequency, intensity, and first location have been produced. Statistical tools such as the chi-square and the Kolmogorov–Smirnov test indicate that there is significant potential predictability of interannual variability of simulated tropical storm frequency, intensity, and first location over most of the ocean basins. The only common point between the nine members of the ensemble is the SST forcing. This implies that SSTs play a fundamental role in model tropical storm frequency, intensity, and first location interannual variability. Although the interannual variability of tropical storm statistics is clearly affected by SST forcing in the GCM, there is also a considerable amount of noise related to internal variability of the model. An ensemble of atmospheric model simulations allows one to filter this noise and gain a better understanding of the mechanisms leading to interannual tropical storm variability.

An EOF analysis of local SSTs over each ocean basin and a combined EOF analysis of vertical wind shear, 850-mb vorticity, and 200-mb vorticity have been performed. Over some ocean basins such as the western North Atlantic, the interannual frequency of simulated tropical storms is highly correlated to the first combined EOF, but it is not significantly correlated to the first EOF of local SSTs. This suggests that over these basins the SSTs have an impact on the simulated tropical storm statistics from a remote area through the large-scale circulation as in observations. Simulated and observed tropical storm statistics have been compared. The interannual variability of simulated tropical storm statistics is consistent with observations over the ocean basins where the model simulates a realistic interannual variability of the large-scale circulation.

1. Introduction

Manabe et al. (1970) detected the presence of tropical disturbances similar to observed tropical storms in a GCM run. Bengtsson et al. (1982), Wu and Lau (1992), and Bengtsson et al. (1995), among others, have described GCM simulations of tropical storm structure, climatology, and interannual variability that have many similarities with observations. Wu and Lau (1992) compared the interannual variability of tropical storm frequency obtained using a single run of an R15 GCM forced by observed SSTs with observed interannual variability. Tsutsui and Kasahara (1996), using the National Center for Atmospheric Research (NCAR) community climate model, demonstrated that tropical storm interannual variability obtained using observed SSTs was of the same order of magnitude as the interannual variability using climatological SSTs. This necessitates the use of ensemble GCM simulations to separate the interannual signal from noise.

Vitart et al. (1997, hereafter V97) used a nine-member ensemble of 10-yr integrations (1979–88) of a GCM forced by observed SSTs to evaluate the interannual frequency of tropical storms. Statistical tools such as the chi-square test were used to measure the potential predictability of the interannual variability of tropical storm frequency. The results of V97 indicated significant potential predictability and predictive skill over the western North Atlantic, the eastern North Pacific, and the western North Pacific. The model displayed less potential predictability over the western North Pacific, the Australian basin, and the South Pacific. The interannual frequency of the ensemble mean was strongly anticorrelated with observations over the south Indian Ocean and the South Pacific. These results of V97 indicate that the GCM is able to produce an interannual variability of tropical storm frequency over most of the basins, but this interannual variability is not always consistent with observations.

Corresponding author address: Dr. F. Vitart, ECMWF, Shinfield Park, Reading, Berkshire RG2 9AX, United Kingdom.
E-mail: nec@ecmwf.int

The only common point between the nine members of the ensemble described in V97 is the observed SST forcing. The potential predictability obtained over most of the ocean basins indicates the strong impact of the SSTs on the interannual variability of the simulated tropical storm frequency. This paper examines whether the SSTs influence simulated tropical storms through a direct local effect or through an indirect dynamical response. In addition, comparison with observations will be presented to better understand the behavior of both simulated and real tropical storms.

Observed tropical storms appear during specific periods of the year and only over specific locations in the Tropics. There is almost no cyclogenesis over the central North Pacific (between 180° and 150°W) or over the eastern South Pacific (east of 120°W), and cyclones over the South Atlantic are nonexistent. The tropical storm interannual variability is large over some basins; for example, over the western North Pacific only 18 tropical storms were detected in 1959 while 39 were detected in 1964. To explain this observed tropical storm climatology and interannual variability, Gray (1968) investigated relationships between tropical storm frequency and large-scale circulation, keying on the position of the ITCZ. Gray (1979) identified six principal large-scale parameters that have an important impact on tropical storm cyclogenesis. From these six parameters, a seasonal genesis parameter was defined that gives values close to the observed tropical storm frequency over most basins for the period 1958–78. This seems to indicate that in observations, the large-scale circulation has an important impact on tropical storm cyclogenesis. The present paper investigates if such a relationship is present in the ensemble simulation.

After a brief presentation of the ensemble simulations in section 2, section 3 presents a description of the parameters used to evaluate the impact of the atmospheric large-scale circulation on simulated tropical storms. In section 4, the potential predictability of the interannual variability of tropical storm first location and maximum intensity is evaluated. The main goal of the present paper is to investigate if there is a relationship between simulated large-scale circulation and simulated tropical storm frequency, maximum intensity, and first position, similar to the one that has been observed and described in Gray (1979). For this purpose, section 5 presents a combined EOF analysis of the simulated large-scale circulation and SSTs over each ocean basin, and the relationship between these combined EOFs and simulated tropical storm statistics is investigated. In section 6, the skill of the ensemble in simulating a realistic interannual variability of tropical storm frequency, intensity, and location is evaluated. In section 7, an EOF analysis similar to the one presented in section 5 is performed on observations from the National Centers for Environmental Prediction (NCEP)–NCAR reanalysis. In this section, the differences between the simulated and observed interannual variability of tropical storm frequency, intensity, and location are investigated.

All the statistics concerning observed tropical storms have been obtained from the National Hurricane Center (in Miami, Florida), the Joint Typhoon Warning Center (in Guam), and Consolidated World-Wide Tropical Cyclones (National Climatic Data Center). Large-scale observed fields are from the NCEP–NCAR 40-yr Reanalysis Project (Kalnay et al. 1996).

2. Description of the experiment

The GCM used in the ensemble simulation was described in detail in Gordon and Stern (1982). A T42 atmospheric model with 18 vertical levels forced by observed SSTs (Gates 1992) has been integrated for 10 yr (1 January 1979–31 December 1988) with nine different initial conditions. The initial conditions were taken from analyses for 12 December 1978–21 January 1979, sampled every 5 days; each of these analyses was then used as an initial condition as if it were the analysis for 1 January 1979. The first year of the ensemble integrations has been discarded in an attempt to eliminate direct effects of the initial conditions.

The parameterization of the atmospheric model includes ''bucket'' hydrology (Manabe 1969); orographic gravity wave drag (Stern and Pierrehumbert 1988); large-scale condensation and moist convective adjustment (Manabe et al. 1965) (both using a condensation criterion of 100%); shallow convection (based on Tiedtke 1988); cloud prediction [interactive with the radiation (Gordon 1992)]; radiative transfer (12-h averaged), which varies seasonally; stability-dependent vertical eddy fluxes of heat, momentum, and moisture throughout the surface layer, the planetary boundary layer, and the free atmosphere (Sirutis and Miyakoda 1990); and $k\nabla^4$ horizontal diffusion. The surface temperatures over land and over sea ice are determined by solving surface heat balance equations (Gordon and Stern 1982).

An objective procedure for tracking model tropical storms (V97) has been applied to the nine-member ensemble. Analysis has been performed for seven ocean basins: the western North Atlantic (WNA), the eastern North Pacific (ENP), the western North Pacific (WNP), the north Indian Ocean (NI), the south Indian Ocean (SI), the Australian Basin (AUS), and the South Pacific (SP) (Fig. 4 in V97).

3. Large-scale parameters

In Gray (1979), six large-scale parameters are related to increased frequency of tropical storm genesis: above-average low-level vorticity and midlevel moisture, conditional instability through a deep layer, warm and deep oceanic mixed layer, weak vertical shear of the horizontal wind, and significant value of the planetary vorticity (observed tropical storms are always located at least a few degrees poleward of the equator). As noted

by Frank (1987), the parameters cited above are not completely independent. In the Tropics, above-average midlevel moisture and conditional instability through a deep layer are strongly correlated with high SSTs, so these two parameters have been discarded in the present study. The planetary vorticity has been discarded because it is the same in the model and the observations and does not present interannual variability. Therefore, three of Gray's parameters have been retained in the present study: the SSTs, the vertical shear of the horizontal wind, and the low-level vorticity. The low-level vorticity is believed to have a fundamental impact on observed tropical storm cyclogenesis through two processes (Frank 1987):

- Ekman pumping to initiate the original disturbance, and
- a reduction of the Rossby radius of deformation. As the energy from the diabatic heating is dispersed radially by gravity waves over a scale comparable to the Rossby radius of deformation, a smaller radius of deformation implies more efficiency and so more favorable conditions for cyclogenesis.

Vertical wind shear also plays a fundamental role in tropical storm cyclogenesis. As discussed by Gray (1968), tropical cyclones form only in the presence of a small vertical shear of the horizontal wind between the lower and upper troposphere. When strong baroclinic conditions prevail, cloud cluster ventilation is strong and enthalpy and moisture cannot be accumulated above the center of the developing storm, preventing pressure falls. Strong vertical wind shear over the central South Pacific is believed to be the primary cause of the lack of observed tropical storms in this region (Gray 1968).

McBride (1981a,b) and McBride and Zehr (1981) have performed composite analyses and case studies of cyclones over the North Atlantic and North Pacific to evaluate the conditions present during the genesis of individual storms. They found that tropical storm formation occurs only when a preexisting convective disturbance enters a large-scale region with above-average cyclonic vorticity at low levels and anticyclonic vorticity at upper levels. So large-scale upper-level vorticity also plays an important role in tropical storm cyclogenesis. For this reason, this parameter has been added to the low-level vorticity and vertical wind shear parameters.

In the present study, the low- and upper-level vorticities are taken to be the vorticity at 850 and 200 mb, respectively, and the vertical wind shear of the horizontal wind has been defined as the magnitude of the difference of the wind at 850 mb and the wind at 200 mb.

4. Potential predictability of simulated tropical storm frequency, first location, and intensity

Over each ocean basin, the number of tropical storms per season has been counted (V97), and statistics on tropical storm intensity and location have been produced. The tropical storm season over the Northern Hemisphere begins in January and ends in December; over the Southern Hemisphere it begins in July and ends in June. From 1 January 1980 through 31 December 1988, there are nine tropical storm seasons over the Northern Hemisphere and eight tropical storm seasons over the Southern Hemisphere.

The maximum 850-mb wind velocity within a 5° radius of the tropical storm center has been chosen to measure the intensity of a tropical storm. The use of the minimum pressure in the center of the tropical storms gives results consistent with those obtained using the maximum wind velocity. The maximum wind velocity has been averaged over all the tropical storms that occur over one basin during one season to define an index of the intensity of storms. This index has been computed over each basin and for each season from 1980 to 1988.

Two indexes have been used to study the interannual variability of the location of tropical storms. The first is the latitude of the first position of tropical storms averaged over all the storms that occur over a basin during one tropical storm season. The second index is the longitude.

In the present study, the ensemble simulation is said to have *potential predictability* if the ensemble distribution of tropical storm number, intensity, or location for a given year can be distinguished from the model ''climatological'' distribution of these quantities in a statistically significant way. In other words, the nine-member ensemble displays potential predictability if the simulation it provides for a given year is statistically different from the simulation produced by randomly selecting nine elements from the model climatological distribution. The model climatological distribution is defined in this study as being the nine-season ensemble distribution for the Northern Hemisphere basins and the eight-season (1981–88) ensemble distribution for Southern Hemisphere basins. This climatological distribution has 81 members in the Northern Hemisphere and 72 members in the Southern Hemisphere.

The tropical storm frequency is a discrete variable, while the indexes for intensity and location are continuous. Therefore, a chi-square test (see V97) has been applied to measure the potential predictability of tropical storm frequency, while a Kolmogorov–Smirnov test (KS test) (Press 1986; Knuth 1981) has been used for intensity and location. The null hypothesis of these statistical tests is that the ensemble distribution for a given year is identical to the climatological distribution. When the statistical tests indicate that the two distributions can be distinguished with a level of confidence larger than 90%, then the ensemble is said to display potential predictability for that given year.

Over the western North Atlantic the significance of the chi-square test applied to the ensemble distribution of tropical storm frequency exceeds 90% in 1980, 1981,

TABLE 1. Significance of the chi-square test (Kolmogorov–Smirnov test) to evaluate the potential predictability of tropical storm frequency (intensity, latitude, and longitude) over the western North Atlantic.

	1980	1981	1982	1983	1984	1985	1986	1987	1988
Frequency	0.94	0.992	0.996	0.26	0.36	0.95	0.92	0.91	0.76
Intensity	0.005	0.09	0.05	0.41	0.35	0.02	0.01	0.67	0.82
Lat	0.68	0.64	0.68	0.999	0.42	0.53	0.88	0.64	0.94
Long	0.83	0.6	0.359	0.99	0.011	0.93	0.80	0.011	0.54

1982, 1985, 1986, and 1987 (Table 1). Over the other ocean basins, the model displays significant potential predictability of tropical storm frequency during most of the years except over the north Indian Ocean (Table 5 in V97). Over the western North Atlantic, the significance of the KS test on tropical storm *intensity* never exceeds 90% (Table 1), so the ensemble does not display potential predictability in simulating the interannual variability of tropical storm intensity over this basin. Over the other basins, the ensemble displays potential predictability of tropical storm intensity over the western North Pacific, the south Indian Ocean, the Australian Basin, and the South Pacific, but not over the eastern North Pacific and the north Indian Ocean (not shown).

The model displays significant potential predictability of tropical storm mean *latitude* during two years (1983 and 1988) over the western North Atlantic (Table 1) and at least one year (which should happen by chance since the level of significance is 90% and nine years are considered) over all the other basins except the north and south Indian Oceans (not shown). Over the western North Pacific, the ensemble displays a particularly strong potential predictability in 1982 and 1988 with simulated tropical storms located significantly more southward in 1982 and significantly more northward in 1988 (Fig. 1).

The model displays significant potential predictability of tropical storm mean *longitude* during two years (1983 and 1985) over the western North Atlantic (Table 1) and at least one year over all the other basins (not shown). An example of strong potential predictability of tropical storm longitude appears over the western North Pacific in 1982, where the simulated tropical storms are located significantly farther eastward than during any other year, particularly 1988 (Fig. 1).

The main goal of the present study on potential predictability is to evaluate if the model is able to simulate an interannual variability of tropical storm statistics dif-

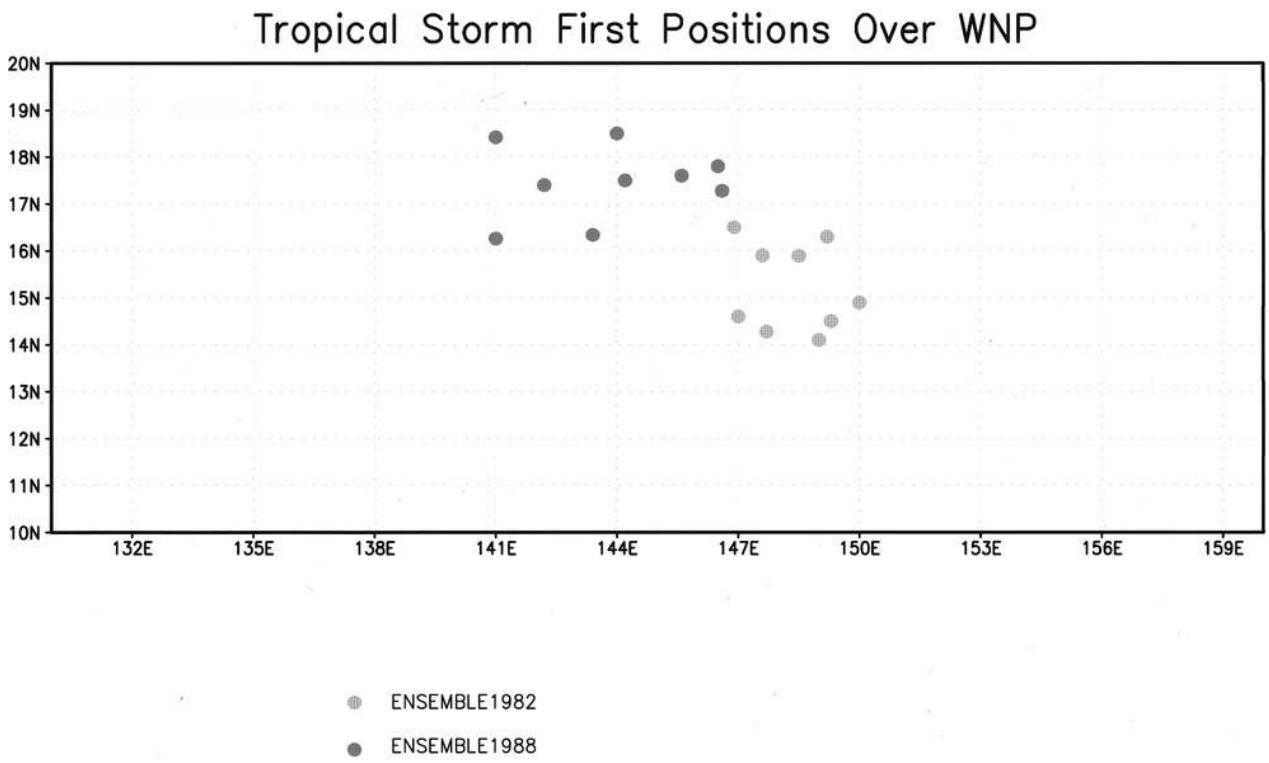

FIG. 1. Mean location of the position where the tropical storms are first detected over the years 1982 (light circles) and 1988 (dark circles). Each circle represents one member of the ensemble.

TABLE 2. Cases where the model simulates an interannual variability that can be distinguished from noise (indicated by an ''X''). The numbers of years where the ensemble displays potential predictability are indicated in parentheses.

	WNA	ENP	WNP	NI	SI	AUS	SP
Frequency	X (6)	X (7)	X (7)	O	X (3)	X (4)	X (2)
Intensity	O	O	X (3)	O	X (2)	X (2)	X (3)
Lat	X (2)	X (3)	X (2)	O	O	X (2)	X (2)
Long	X (2)	X (2)	X (2)	X (3)	X (2)	X (2)	X (2)

ferent from noise. In cases where there is no potential predictability during all the years of the study—for instance, the tropical storm intensity over the western North Atlantic (Table 1)—the interannual variability produced by the model may not be distinguished from noise. Therefore, these cases have been discarded from further consideration in the present paper. In addition, the tropical storm frequency over the north Indian Ocean basin has been discarded, although the model displays potential predictability in simulating its interannual variability during two years. This is due to the fact that in the next section of this paper, only the mean of the ensemble will be considered, and the mean number of simulated tropical storms over the north Indian Ocean is nearly the same during the nine years of the ensemble (the significant potential predictability in 1980 and 1987 over this basin originates from a difference in the spread of the ensemble). This indicates that the measure of potential predictability should not be restricted to a measure of the spread of the ensemble but must take into account the differences in the mean. Table 2 indicates the cases that will be considered in the next sections (indicated with an ''X'') and those that have been discarded (indicated with ''O'').

The cases that have not been discarded present an interannual variability that is different from noise. The only common point between the nine members of the ensemble is the SSTs. It can then be concluded that the SSTs have a significant impact on the simulated tropical storm statistics over the basins indicated by an ''X'' in Table 2. The principal goal of the next section is to determine if the simulated tropical storms are affected only by local SSTs or if they are affected by SSTs located in a remote area.

5. EOF analysis of SSTs and simulated large-scale circulation

The present section presents in detail only results concerning tropical storm frequency over the western North Atlantic. Results for other basins and other statistics are presented when they are particularly relevant to the discussion. The focus on tropical storm frequency is mostly motivated by the stronger potential predictability obtained with frequency rather than by intensity, longitude, and latitude (Table 2).

Over each ocean basin, the SSTs have been averaged over the period corresponding to the tropical storm season (June–October over the western North Atlantic, eastern North Pacific, and western North Pacific; May, June, October, and November over the North Indian Ocean; December–April over the Southern Hemisphere). An EOF analysis (referred to as SST EOFs hereafter) has been performed on the interannual variability of the averaged SSTs for each basin from 1980 to 1988. All the EOF analyses displayed in the present paper use a *correlation* matrix as an input matrix. The interannual variances of SSTs and large-scale circulation display strong variations in amplitude from one grid point to another. This fact and the requirement that the grid point must have an equal contribution to the EOFs motivated the use of a correlation matrix.

Over the WNA, the SST EOF1 represents 57.8% of the total variance, and its amplitude is almost homogeneous over the entire basin (Fig. 2). The WNA SST EOF2 represents only 12.3% of the total variance; therefore, only the SST EOF1 will be discussed.

The interannual variability of the simulated WNA tropical storm number (Fig. 3a) is not significantly correlated (Table 3) to the SST EOF1 time series (Fig. 3b). Therefore, one can confidently conclude that the local SSTs do not have a significant impact on the simulated WNA tropical storm frequency during the period 1980–88. The significant potential predictability of WNA tropical storm frequency can be explained only by the impact of SSTs from a remote region, and this impact must be through the large-scale circulation. To verify this hypothesis, a combined EOF analysis (referred to as CEOFs hereafter) has been performed on the simulated vertical wind shear, 850-mb vorticity, and 200-mb vorticity, averaged over the period corresponding to the tropical storm season for each basin separately. The sign of the CEOF1 time series has been adjusted such that it is positively correlated to the SSTs averaged over the NINO3 region (from 5°N to 5°S and from 90°W to 150°W). The interannual variability of SSTs over the NINO3 region will hereafter be referred to as the ENSO index.

The WNA CEOF1 represents 37.4% of the total variance. The linear correlation between the CEOF1 time series (Fig. 3a) and the interannual frequency of WNA tropical storms is -0.87 (99% significance). This further supports the hypothesis that the WNA tropical storm frequency simulated by the GCM is primarily constrained by the large-scale atmospheric circulation rather than by the local WNA SSTs.

The linear correlation between the CEOF1 time series and the ENSO index is 0.79 (99% significance), which demonstrates that CEOF1 is related to the impact of ENSO on the WNA large-scale circulation. Therefore, it can be concluded that the interannual frequency of tropical storms over the western North Atlantic is mostly constrained by the interannual variability of SSTs related to ENSO during the period 1980–88. This may be confirmed by the significant linear correlation between

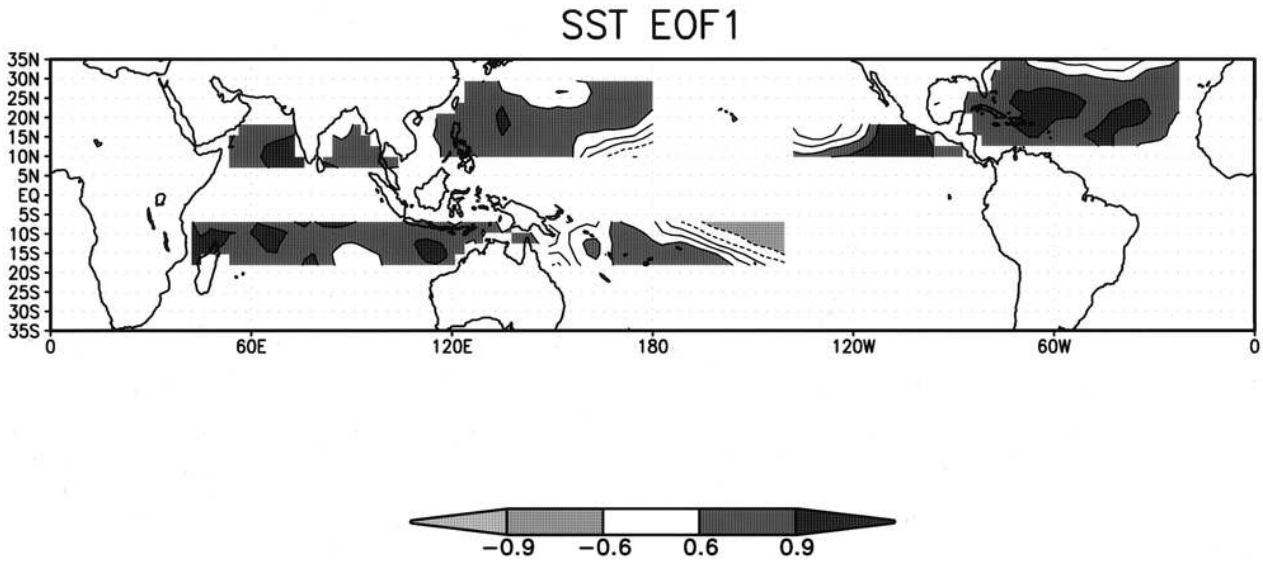

FIG. 2. EOF1 of the interannual variability of SSTs during the period 1980–88. SSTs have been averaged over the tropical storm season over each ocean basin. The figure has been scaled to show the correlations between the EOF1 time series and the interannual variability of SSTs at the grid points. Contours are displayed with an increment of 0.3, and dashed lines represent negative values.

the interannual frequency of simulated WNA tropical storms and the ENSO index (0.84 with 99% significance). WNA SSTs are not related to ENSO since they are not significantly correlated to the ENSO index (Table 4). Therefore, the impact of SSTs on the WNA simulated tropical storms is a remote impact through the large-scale circulation.

Figure 4 (Fig. 5) displays the CEOF1 (CEOF2) pattern for the period 1980–88. The sign of CEOF1 and CEOF2 has been chosen such that its time series over each ocean basin is positively correlated to the ENSO index. Over the western North Atlantic, during El Niño years, the ensemble simulates more intense vertical wind shear, less anticyclonic 200-mb vorticity, and less cyclonic 850-mb vorticity over the western part of the basin where most of the simulated tropical storms occur. All these are less favorable to tropical storm genesis and development, which may explain the negative correlation between the CEOF1 time series and the frequency of WNA tropical storms.

Over all the other basins except the south Indian Ocean, the linear correlation between the frequency of simulated tropical storms and the CEOF1 time series for that basin is always strong and significant (Table 3). Over the south Indian Ocean, the CEOF2 time series displays the strongest correlation with storm frequency. Over the south Indian Ocean, most of the simulated tropical storms occur in the western part of the basin, where CEOF2 explains more of the variance.

Over the western North Pacific and the Australian Basin, the local SST EOF1 time series is not significantly correlated to the frequency of tropical storms (Table 3). Over these two basins, conclusions similar to those obtained for the western North Atlantic can be applied: local SSTs have no significant impact on the tropical storm frequency, which is mostly constrained by the large-scale circulation. Over the eastern North Pacific and the South Pacific, the interannual variability of local SSTs is significantly correlated to the CEOF1 time series and to the interannual frequency of tropical storms. The fact that the linear correlations are more significant with the CEOF1 time series than with the SST EOF1 time series over all the ocean basins except the south Indian Ocean is a possible indication that the interannual variability of tropical storms over these basins is mostly constrained by the vertical wind shear, low-level vorticity, and 200-mb vorticity. Over the south Indian Ocean, the SST EOF1 and CEOF2 time series are not significantly correlated (correlation of 0.48 with a significance of 78%), but both are significantly correlated to the interannual variability of tropical storms (Table 3; if this study were a prediction problem, two uncorrelated predictors would have favorable implications for forecasting).

Over all ocean basins except the Australian Basin and the south Indian Ocean, the CEOF1 time series is significantly correlated to the ENSO index (Table 4). The ENSO index may vary from one basin to another, since it has been defined as the SSTs averaged over the NINO3 region and over the tropical storm season of the ocean basin considered. The linear correlations between the simulated CEOF2 time series over the south Indian Ocean and the SSTs (Fig. 6a) do not allow definitive conclusions about an impact of SSTs on the simulated CEOF2 over the south Indian Ocean, since no large pattern of significant correlation can be observed. The simulated CEOF1 time series over the Australian Basin

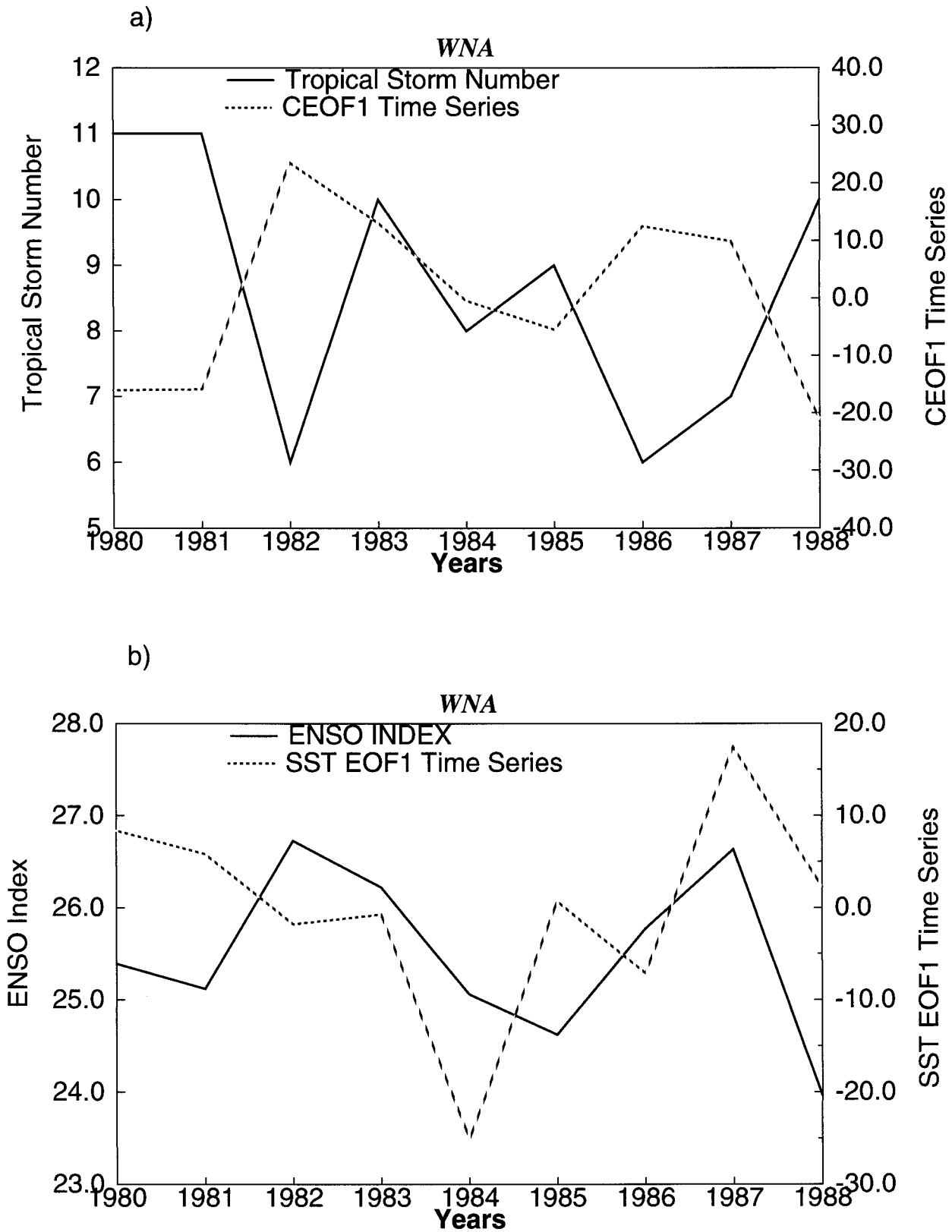

FIG. 3. (a) Tropical storm number simulated by the ensemble of GCM integrations and CEOF1 time series over the western North Atlantic from 1980 to 1988. (b) ENSO index and SST EOF1 time series over the western North Atlantic from 1980 to 1988.

TABLE 3. Linear correlation for each ocean basin between the interannual variability of tropical storm frequency and SST EOF1, simulated CEOF1 and CEOF2 time series. Significance levels are in parentheses.

	WNA	ENP	WNP	SI	AUS	SP
SST EOF1	0.26 (50.0)	0.71 (96.7)	0.39 (70.0)	0.75 (96.8)	−0.44 (72.4)	0.72 (95.6)
CEOF1	−0.87 (99.8)	0.90 (99.9)	−0.88 (99.8)	0.56 (85.1)	−0.90 (99.8)	−0.88 (99.7)
CEOF2	−0.30 (58.3)	−0.07 (14.2)	−0.41 (72.7)	0.77 (97.7)	−0.13 (24.1)	0.39 (66.0)

is significantly correlated with the SSTs over the west tropical Pacific and east tropical Indian Ocean (Fig. 6b).

In summary, the simulated tropical storm frequency over the western North Atlantic and the western North Pacific is mainly influenced by ENSO through the large-scale circulation. ENSO has an impact on the simulated tropical storm frequency over the eastern North Pacific and the South Pacific through both the large-scale circulation and the local SSTs. SSTs located in the western part of the North Pacific and the eastern part of the tropical Indian Ocean have an impact on the simulated tropical storms over the Australian Basin. The south Indian Ocean is the only ocean basin where the local SSTs have a significant impact, distinct from the large-scale circulation, on the simulated tropical storm frequency.

The analyses for the three other tropical storm statistics (intensity, longitude, and latitude) give similar conclusions concerning the predominant role of the large-scale circulation on the simulated tropical storms. For example, the interannual variability of tropical storm *intensity* over the western North Pacific displays a stronger linear correlation with the CEOF1 time series (−0.91 with a significance of 99.9%) than with the local SST EOF1 (0.59 with a significance of 90%). In addition, the interannual variability of tropical storm *location* simulated by the GCM is consistent with the CEOF1 or CEOF2 patterns. Two examples may illustrate this last point.

- Over the eastern North Pacific, the model simulates a southeastward shift of tropical storm location during El Niño years. This is roughly consistent with the CEOF1 pattern (Fig. 4), which has lower wind shear and more anticyclonic 200-mb vorticity (both more favorable for tropical storm genesis) in the west and south parts of the basin during El Niño years.
- Over the western North Pacific, the 850-mb vorticity in CEOF1 presents a north-south dipole (Fig. 4), which may explain the southward shift of simulated tropical storms during El Niño years and northward shift during the 1988 La Niña year.

6. Comparison between simulated and observed tropical storm statistics

As examples of the skill of the model to simulate realistic interannual variability of tropical storm statistics, Figs. 7 and 8 display the ensemble distribution of simulated tropical storm latitude and longitude over the western North Pacific along with the observations. To evaluate the realism of the tropical storm simulation, linear correlations between simulated (ensemble mean) and observed tropical storm frequency (already presented in V97), intensity, longitude, and latitude have been performed (Table 5). Results are presented only for basins where the model displays potential predictability (see section 4).

As discussed in V97, the model appears to have skill in simulating the interannual variability of tropical storm *frequency* over the western North Atlantic, the eastern North Pacific, the western North Pacific, and the Australian Basin but displays significant negative correlations over the south Indian Ocean and the South Pacific. It appears that over basins where the model displays potential predictability in simulating tropical storm *intensity*, the interannual variability of intensity is negatively correlated with observations, particularly over the western North Pacific, the south Indian Ocean, and the Australian Basin (Table 5). The EOF analysis presented in section 7 gives a possible explanation of some of these significant anticorrelations.

The model displays some skill in simulating tropical storm *latitude* interannual variability particularly over the eastern North Pacific and, to a lesser extent, over the western North Pacific and the Australian Basin (Table 5). Over the western North Atlantic, the linear correlation is negative, mainly because of an unrealistic tropical storm location and frequency in 1983. In 1983, the model simulates a large number of tropical storms in the southern part of the Gulf of Mexico, which did not appear in the observations.

Over the ocean basins located in the Northern Hemisphere, the model displays skill in simulating the interannual variability of tropical storm *longitude* with a

TABLE 4. Linear correlation between the ENSO index and SST EOF1, simulated CEOF1 and CEOF2 time series. Significance levels are in parentheses.

	WNA	ENP	WNP	SI	AUS	SP
SST EOF1	0.22 (42)	0.92 (99.9)	−0.52 (85)	0.87 (99)	0.57 (86)	−0.98 (99)
CEOF1	0.79 (99)	0.74 (98)	0.85 (99)	0.31 (51)	0.22 (40)	0.96 (99)
CEOF2	−0.21 (42)	0.38 (70)	0.11 (23)	0.42 (70)	0.63 (90)	0.03 (5)

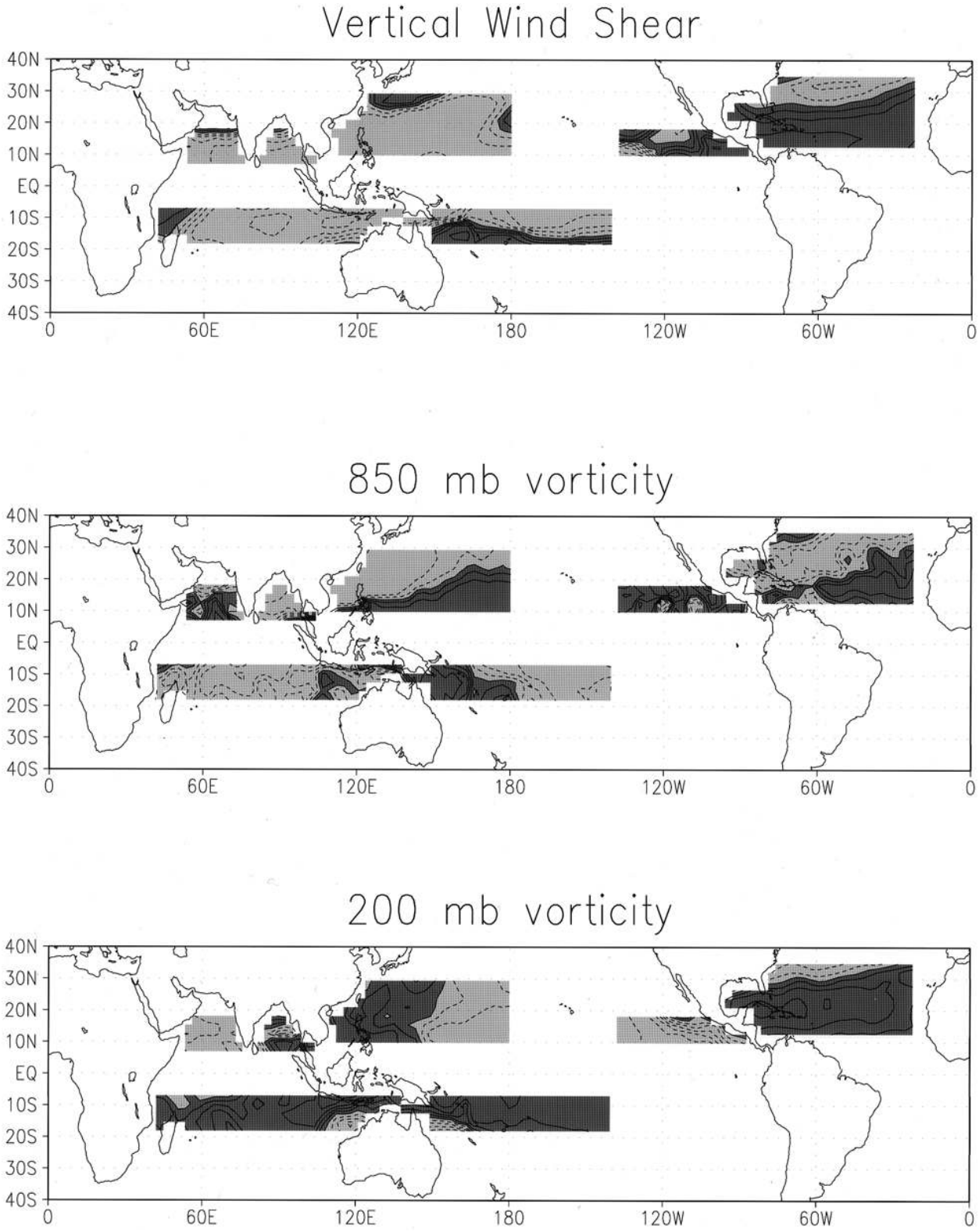

FIG. 4. CEOF1 pattern for simulated vertical wind shear, 850-mb vorticity, and 200-mb vorticity calculated over each ocean basin separately during the tropical storm season. Light shaded areas represent negative values and dark shaded areas represent positive values. The figure has been scaled to show the correlations between the CEOF1 time series and the interannual variability of vertical wind shear, 850-mb vorticity, and 200-mb vorticity at the grid points. Contours are displayed with an increment of 0.3, and dashed lines represent negative values.

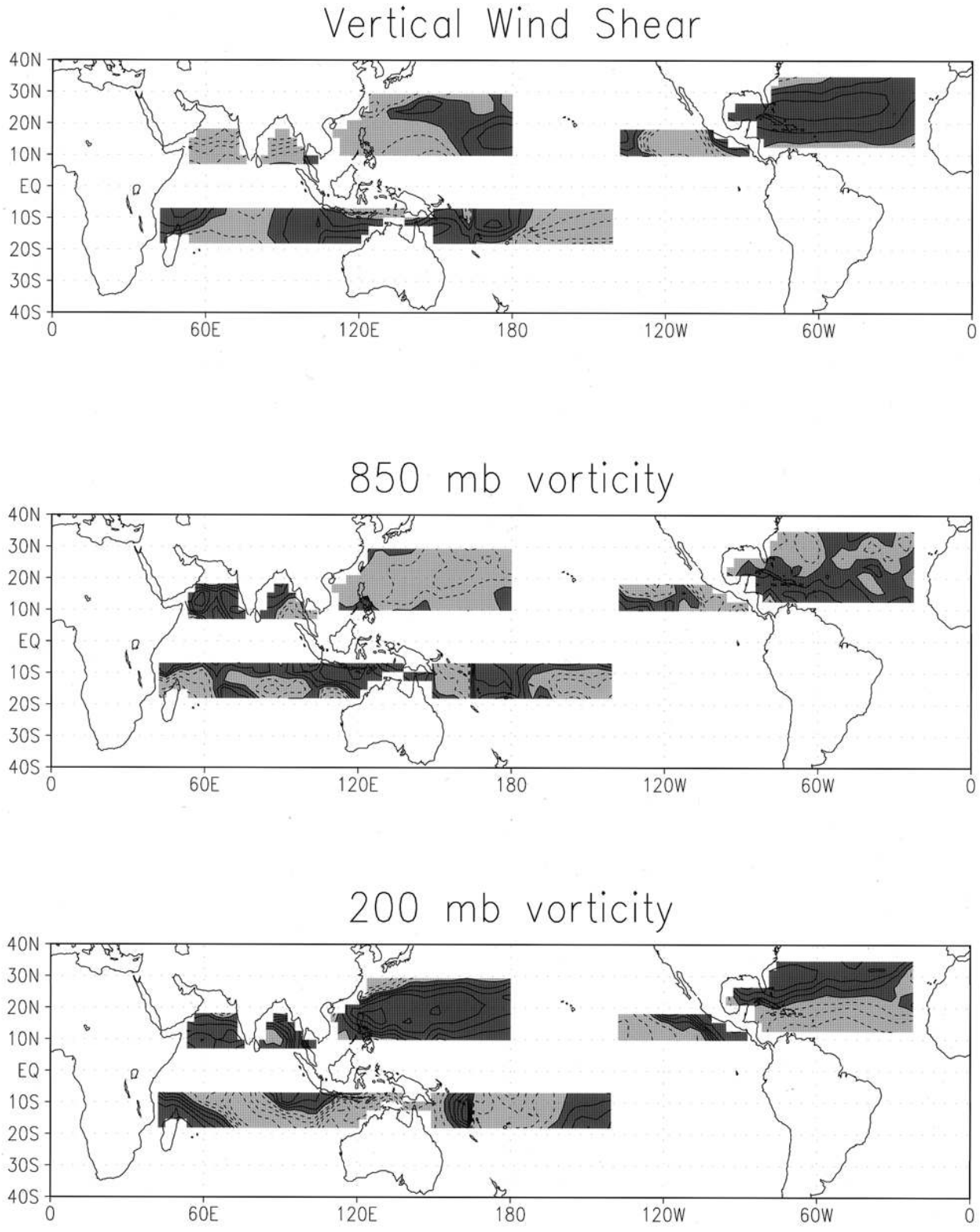

FIG. 5. As in Fig. 4, but for CEOF2.

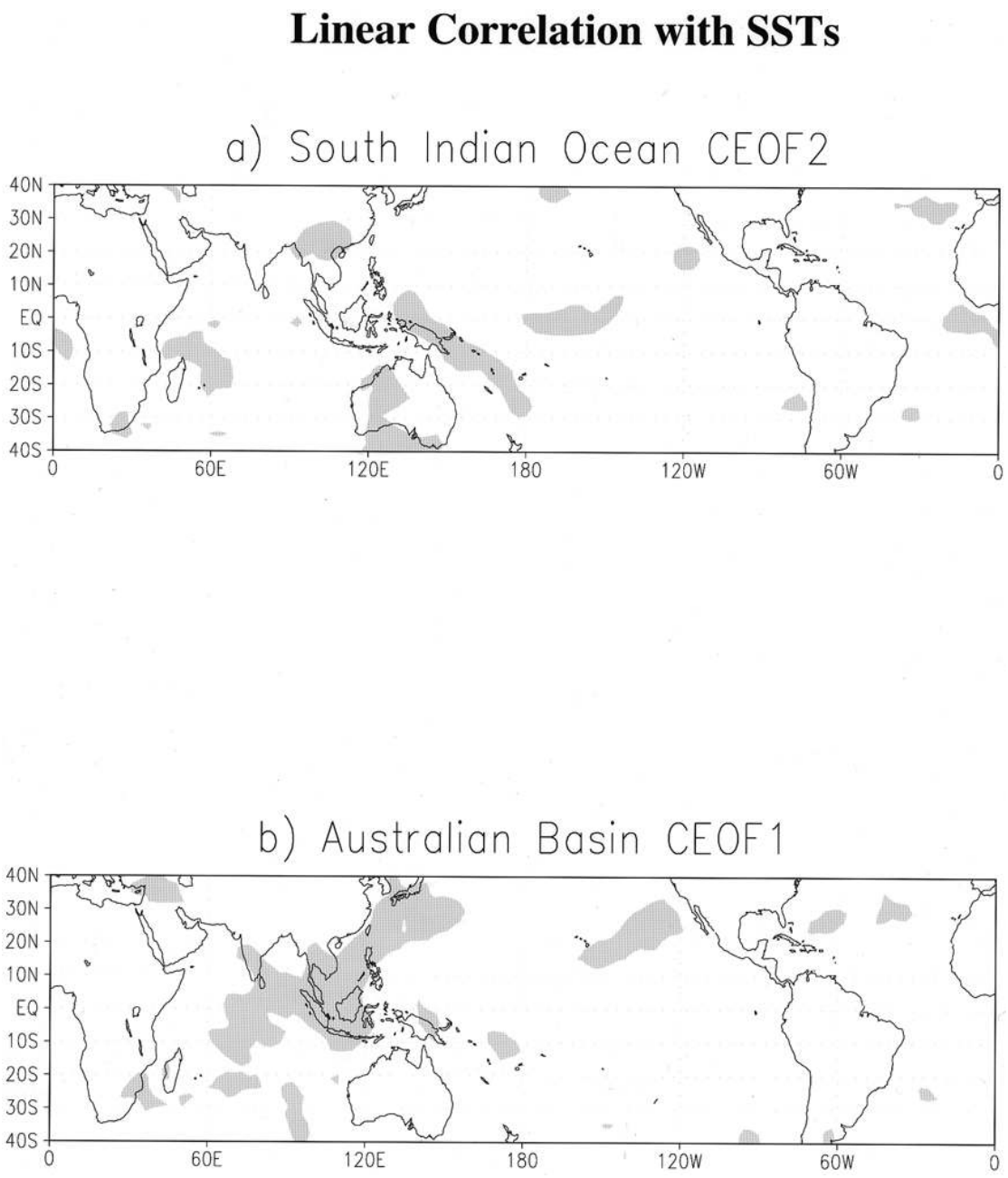

FIG. 6. Correlation of SST time series for the period 1980–88 to (a) south Indian Ocean CEOF2, (b) Australian Basin CEOF1 time series. The shaded areas represent the regions where the linear correlation has a significance larger than 90%.

correlation larger than 0.5. On the other hand, over the basins in the Southern Hemisphere, the correlations are negative and not significant (Table 5).

In summary, the model displays more skill in simulating realistic tropical storm statistics over the Northern Hemisphere than over the Southern Hemisphere. Over the Southern Hemisphere, the majority of the linear correlations between the interannual variability of observed and simulated tropical storm statistics are negative. The next section presents some possible explanations of the negative correlations between the interannual variability of simulated and observed tropical storm statistics over some basins.

7. EOF analysis of observed large-scale circulation and comparison with the ensemble simulation

It has been seen in section 5 that the large-scale circulation seems to have an impact on the simulated tropical storms, consistent with observations by Gray

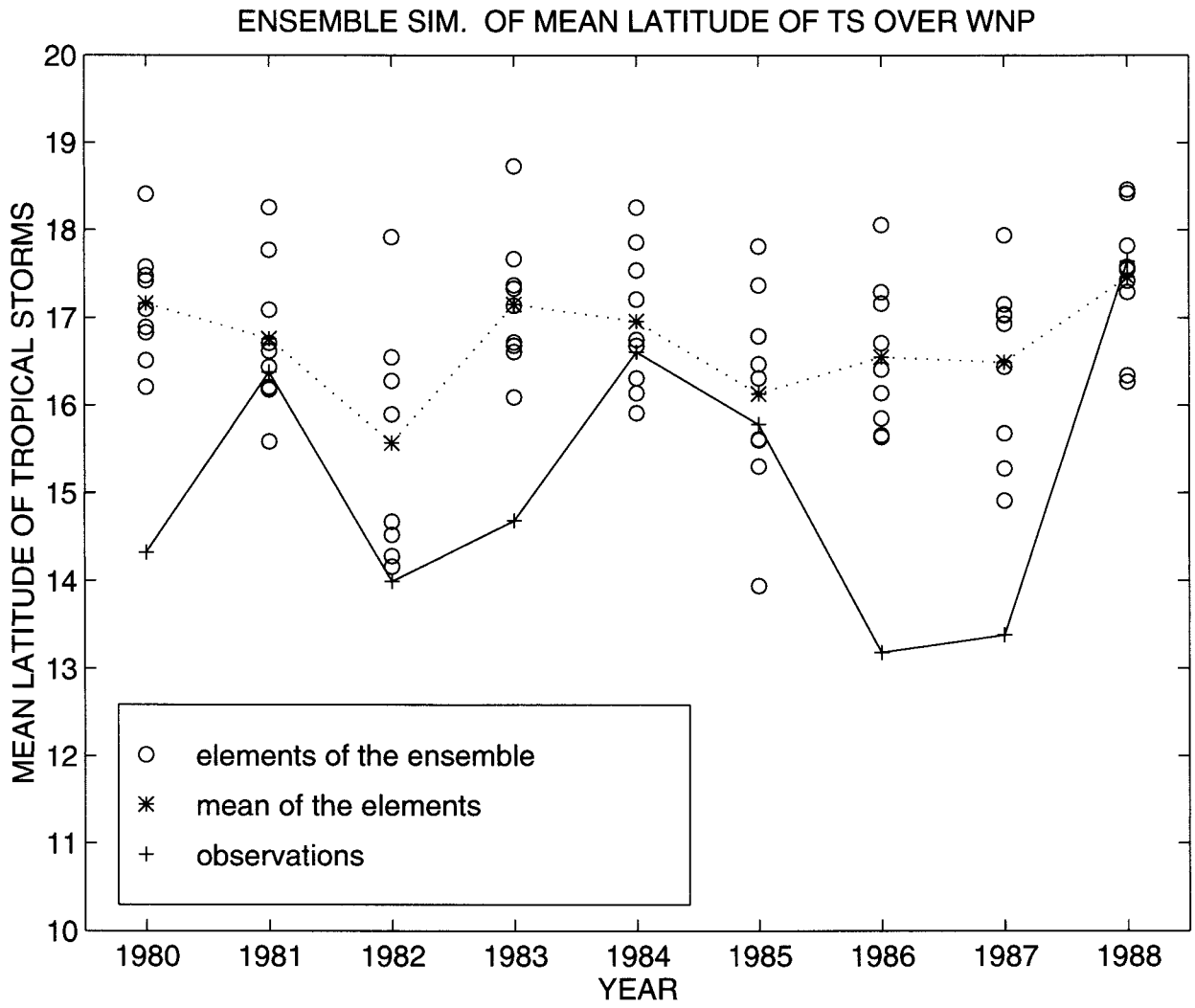

FIG. 7. Ensemble simulation of latitude of first position of tropical storms averaged over all the tropical storms over the western North Pacific. The solid line represents observed tropical storm mean latitude of the first position. The dotted line represents the ensemble mean tropical storm mean latitude. Each circle represents the tropical storm mean latitude of one element of the ensemble.

(1979). Although the SSTs used to force the model may contain significant errors (particularly over the Southern Hemisphere), it is more likely that differences between simulated and observed large-scale circulations are the primary cause of the differences between simulated and observed tropical storm statistics. To investigate this possibility, an EOF analysis similar to the one presented in section 5 has been performed using NCEP–NCAR reanalysis data. Comparing the observed and simulated CEOFs may indicate if the skill of the ensemble in simulating the interannual variability of tropical storm frequency or location over some basins (e.g., the western North Atlantic) is happenstance or if it is based on a consistent physical mechanism. The sign of the observed CEOF1 time series has been adjusted such that it is positively correlated to the ENSO index (NINO3 SSTs).

Over the WNA, the model simulates a realistic interannual variability of tropical storm frequency with a linear correlation with observations of 0.56 (Table 5). The local SSTs do not seem to have a significant impact on the frequency of observed tropical storms (Table 6), but the observed CEOF1 time series is significantly correlated to the frequency of observed tropical storms over this basin (Table 6 vs Table 3). The strong linear correlation between the observed CEOF1 time series and the ENSO index over WNA (Table 7 vs Table 4) implies that the observed CEOF1 represents the impact of ENSO on the observed large-scale circulation over WNA. During El Niño years, the observed vertical wind shear is more intense, the 850-mb vorticity more anticyclonic, and the 200-mb vorticity more cyclonic over the main tropical storm development region (south of 20°N; Fig. 9). Gray (1984) attributed the reduction of observed WNA tropical storms during El Niño years to these unfavorable conditions for tropical storm devel-

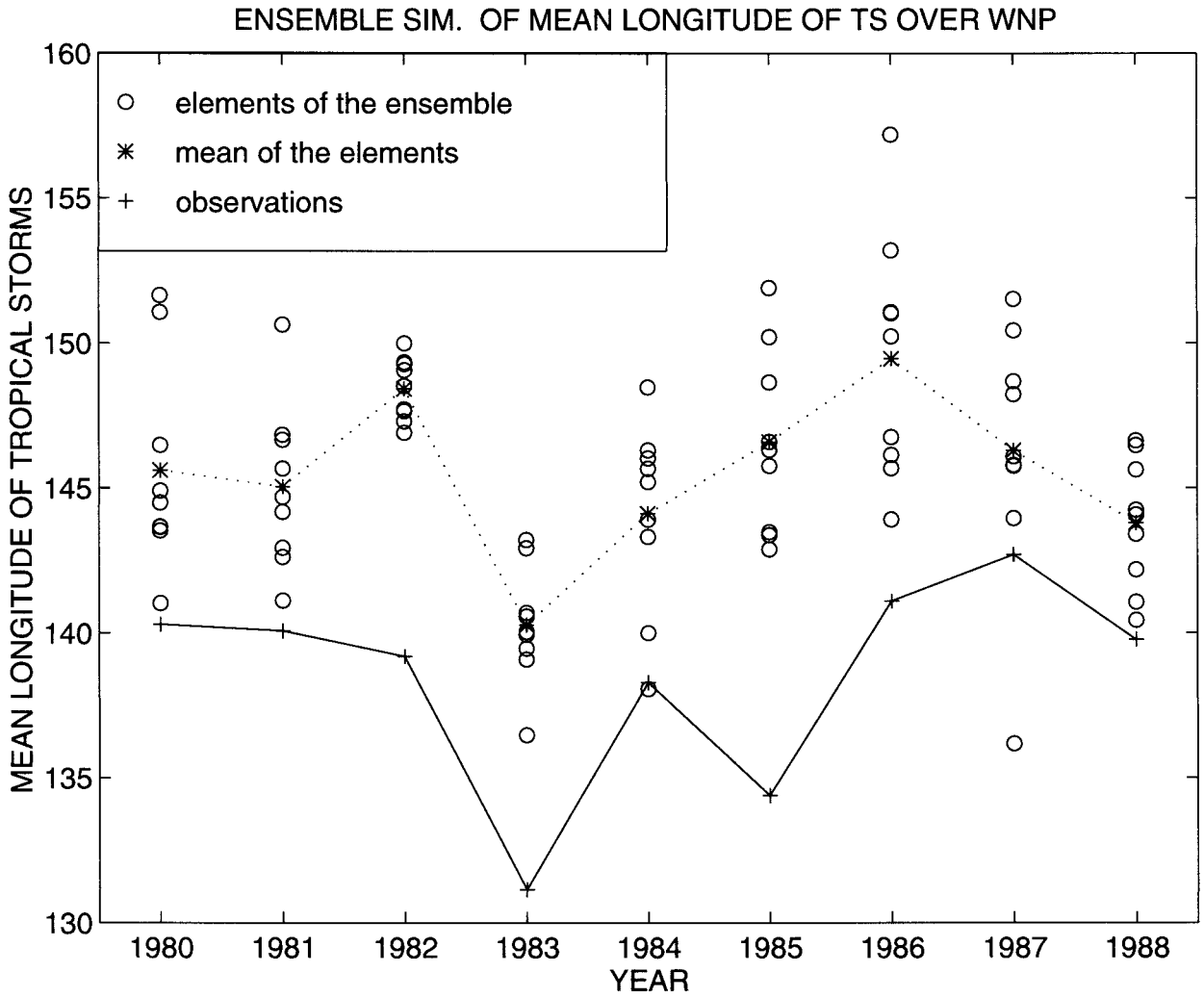

FIG. 8. As in Fig. 7, but for mean longitude.

opment. The impact of ENSO on simulated tropical storms has been described in section 5 and is consistent with the mechanism described above for observations. The simulated and observed CEOF1 patterns over the western North Atlantic display strong similarities (Fig. 9 vs Fig. 4). The simulated 850-mb vorticity pattern in the eastern Atlantic is different from observations, but as the majority of simulated tropical storms occur in the western Atlantic, this has no significant impact on the simulated tropical storm frequency. In observations, there are strong dipoles in the vertical wind shear and 200-mb vorticity patterns between regions north and south of 20°N. This dipole may explain the reduction of observed tropical storms south of 20°N and the increase north of 20°N during El Niño years (Gray 1984) over WNA. The ensemble simulates a dipole structure in both fields, but with a much weaker increase of vertical wind shear in the northern part of the basin (Fig. 9 vs Fig. 4). Therefore, the impact of ENSO over this basin is more homogeneous in the model than in ob-

TABLE 5. Linear correlation between simulated and observed tropical storm frequency, intensity, latitude, and longitude. Significance levels are in parentheses. Results are presented only when the model displays potential predictability.

	WNA	ENP	WNP	NI	SI	AUS	SP
Frequency	0.56 (88.3)	0.55 (87.5)	0.66 (94.5)	—	−0.66 (92.5)	0.57 (85.9)	−0.77 (97.7)
Intensity	—	—	−0.78 (98.8)	—	−0.63 (90.6)	−0.63 (90.6)	−0.10 (18.6)
Lat	−0.37 (67.3)	0.79 (98.9)	0.50 (82.9)	—	—	0.49 (78.2)	0.40 (67.4)
Long	0.54 (86.6)	0.86 (99.9)	0.60 (91.2)	0.52 (84.9)	−0.26 (46.6)	−0.37 (63.3)	−0.14 (25.9)

TABLE 6. Linear correlation for each ocean basin between the interannual variability of observed tropical storm frequency and SST EOF1, observed CEOF1 and CEOF2 time series. Significance levels are in parentheses.

	WNA	ENP	WNP	NI	SI	AUS	SP
SST OEF1	−0.13 (26.1)	0.46 (78.7)	0.002 (0.6)	0.34 (62.3)	−0.70 (94.7)	−0.47 (76.0)	−0.98 (99.9)
CEOF1	−0.60 (91.3)	0.44 (76.4)	0.47 (80.1)	0.11 (22.2)	0.19 (34.8)	−0.77 (97.5)	0.81 (98.6)
CEOF2	−0.13 (26.1)	−0.07 (14.5)	−0.71 (96.8)	0.48 (80.9)	−0.75 (96.8)	0.04 (8.8)	−0.06 (11.2)

servations, and that may explain the stronger impact of ENSO on simulated tropical storms than on observed tropical storms (this is also due to the fact that the ensemble filters a lot of noise that is still present in observations).

The skill of the ensemble in simulating a realistic WNA tropical storm frequency is probably not a coincidence but is apparently based on a somewhat realistic simulated impact of ENSO on the WNA large-scale circulation. Similar arguments can be applied to the other basins and other statistics for which simulated and observed interannual variability are highly correlated.

There remain many significant differences between the ensemble simulation and observations that require an explanation. Two cases of particularly unrealistic simulations will be discussed: the interannual variability of tropical storm frequency over the south Indian Ocean and that over the South Pacific.

Over the south Indian Ocean, local SSTs seem to have an impact on the simulated tropical storm frequency (section 5). These local SSTs are significantly positively correlated to the ENSO index (Table 4), so during El Niño years, the model simulates more tropical storms. The impact of ENSO on the simulated large-scale circulation over the south Indian Ocean is not significant for CEOF1 and CEOF2 (Table 4). In observations, the observed CEOF2 has a time series positively significantly correlated to the ENSO index (Table 7), and its patterns (Fig. 10) indicate more positive (so more anticyclonic) 850-mb vorticity during El Niño years north of 15°S. This represents unfavorable conditions for tropical storm development in the region of observed tropical storm genesis and, therefore, is conducive to a reduction of tropical storm frequency during El Niño years. ENSO seems to have a significant impact on simulated tropical storms through local SSTs and on observed tropical storms through the large-scale circulation. These different mechanisms may explain the significant anticorrelation between simulated and observed tropical storm frequency over the south Indian Ocean (Table 5).

Over the south-central Pacific, the observed vertical wind shear is usually very intense during the tropical storm season and creates unfavorable conditions for tropical storm genesis (Gray 1968). In the simulation, the vertical wind shear over the south-central Pacific is much weaker than in observations. This may explain the presence of simulated tropical storms over this region where tropical storms are not observed. In observations, tropical storms are located in the northwestern part of the basin, where the observed CEOF1 pattern displays favorable conditions for tropical storms genesis and development during El Niño years (more cyclonic 850-mb vorticity and more anticyclonic 200-mb vorticity) (Fig. 9). This may explain the increase of observed tropical storm frequency during El Niño years. On the other hand, most of the simulated tropical storms appear in the southern part of the basin (south of 15°S), where the model simulates an increase of vertical wind shear during El Niño years, which reduces the number of simulated tropical storms. Therefore, the significant anticorrelation between the interannual variability of simulated and observed tropical storms over the South Pacific may be explained by the presence of simulated tropical storms in the south-central Pacific, due to a flaw in the simulated large-scale circulation.

The significant anticorrelation between simulated and observed tropical storm *intensity* (Table 5) over the western North Pacific, the south Indian Ocean, and the Australian Basin cannot be entirely explained by the present CEOF analysis. Therefore, it is possible that differences in the physics of the simulated and observed tropical storms are causing such significant anticorrelations for intensity.

In summary, the unrealistic interannual variability of tropical storm statistics over some of the basins, particularly over the Southern Hemisphere, seems to have its origin in unrealistic large-scale circulation. An improvement in the large-scale circulation of the GCM should increase the skill of the ensemble in simulating a realistic interannual variability of tropical storm frequency and location.

8. Conclusions

The interannual variability of simulated tropical storm statistics contains large amounts of noise, which can be

TABLE 7. Linear correlation between ENSO index and observed CEOF1 and CEOF2 time series. Significance levels are in parentheses.

	WNA	ENP	WNP	NI	SI	AUS	SP
CEOF1	0.73 (97.4)	0.75 (98.2)	0.27 (51.7)	0.75 (98)	0.25 (46)	0.83 (98.9)	0.87 (99.5)
CEOF2	0.08 (16.6)	−0.43 (75.9)	0.65 (94.5)	0.02 (5.56)	0.76 (97)	−0.04 (15.6)	−0.18 (34)

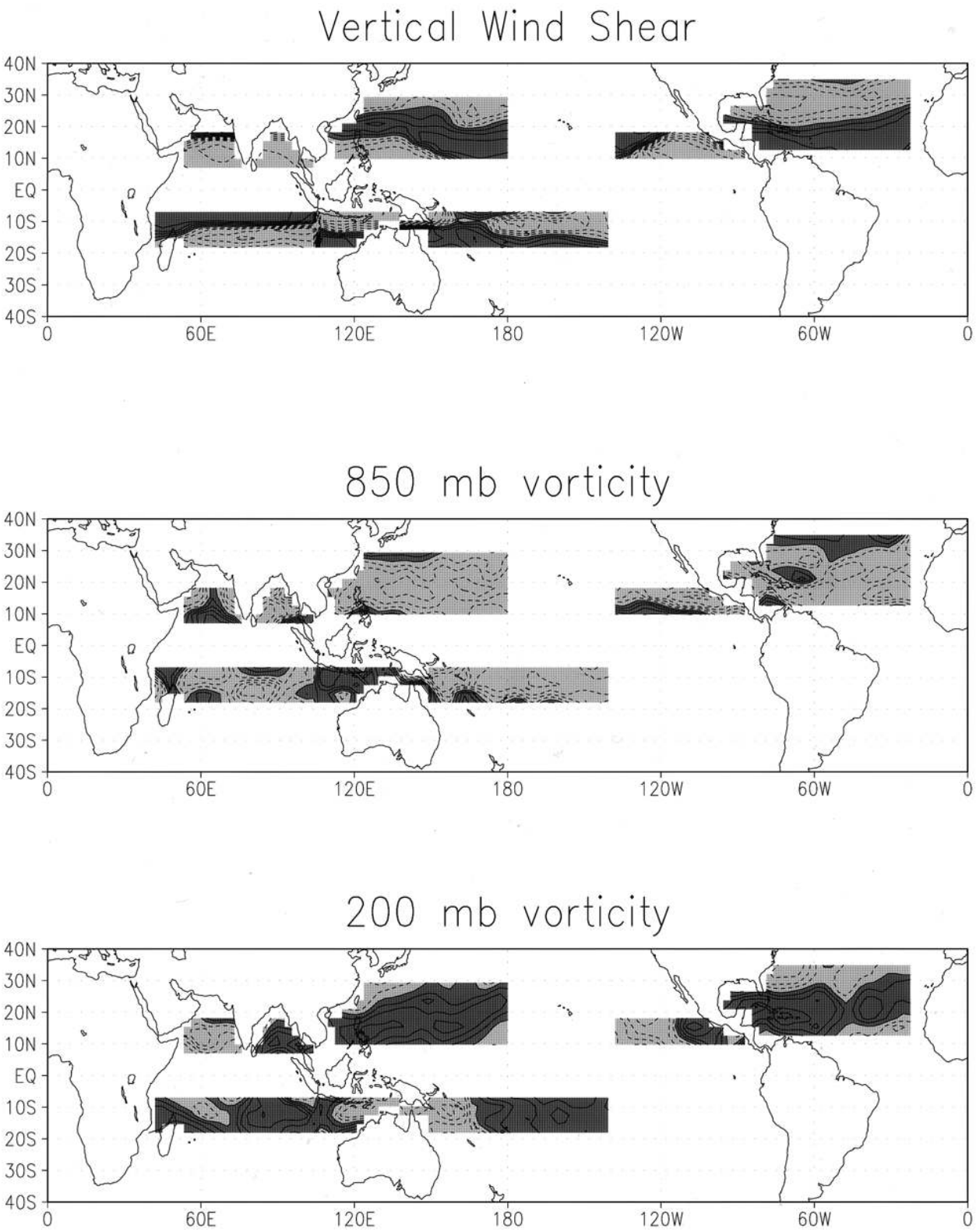

FIG. 9. As in Fig. 4, but for observations.

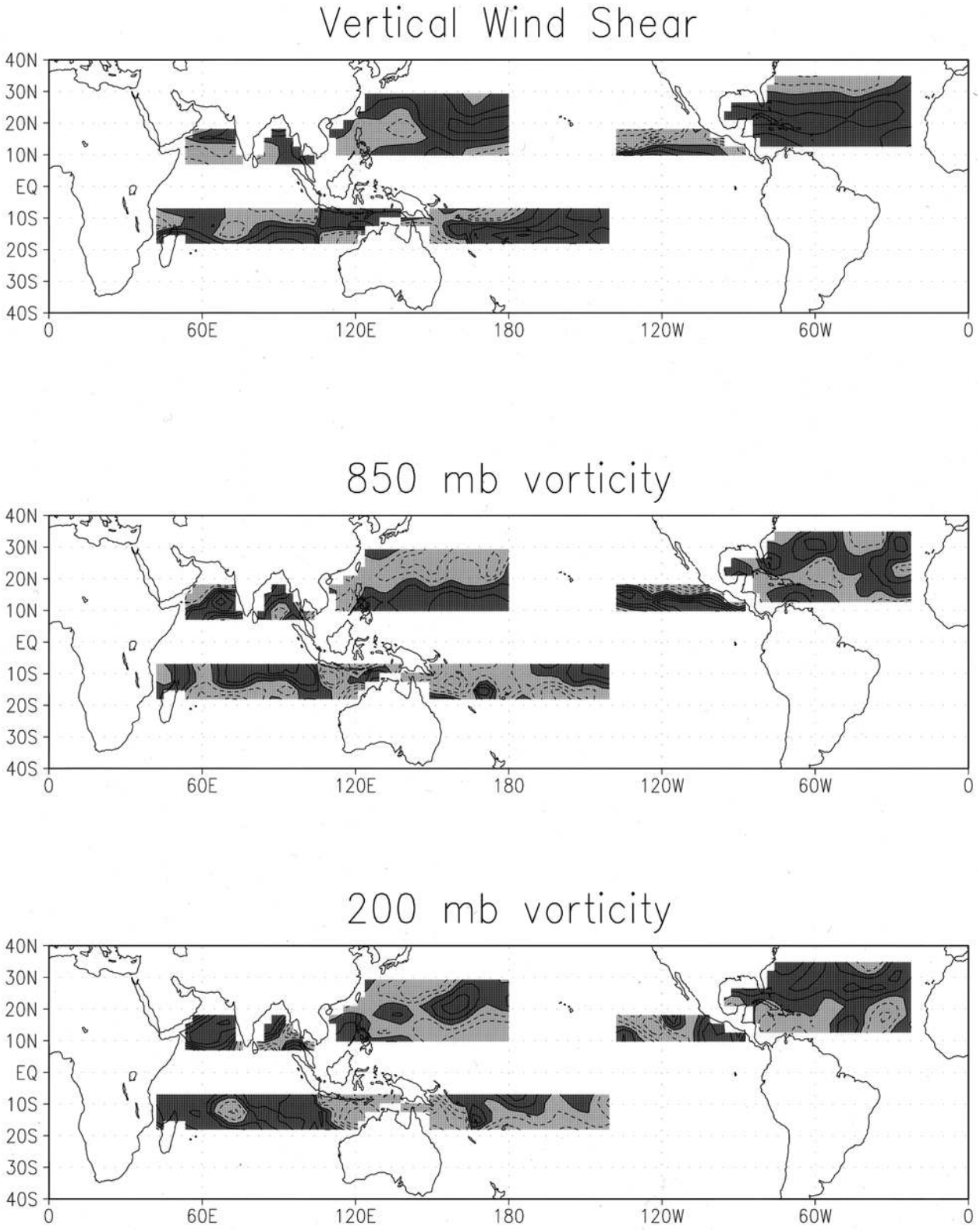

FIG. 10. As in Fig. 5, but for observations.

TABLE 8. Linear correlation between the tropical storm frequency and the simulated CEOF1 time series for each member of the ensemble and for the mean of the ensemble over the western North Atlantic. Significance levels are in parentheses.

Expt. 1	Expt. 2	Expt. 3	Expt. 4	Expt. 5	Expt. 6	Expt. 7	Expt. 8	Expt. 9	Mean
0.04 (10)	−0.55 (88)	−0.54 (87)	−0.61 (92)	−0.13 (92)	−0.42 (74)	−0.81 (99)	−0.13 (27)	−0.78 (98)	−0.87 (99)

filtered by the use of an ensemble. Therefore, the use of an ensemble greatly facilitates evaluating the impact of the simulated large-scale circulation on the simulated tropical storm statistics. The linear correlations obtained by using the nine-member ensemble are much more significant than the linear correlations obtained with a single GCM run (Table 8). Since observations contain some noise, the linear correlations are usually less significant in observations than in the ensemble. Although the signal obtained with the ensemble is not always very realistic, it is a good way to understand the physical mechanisms that may explain the statistics of the interannual variability of simulated tropical storm parameters.

The model displays potential predictability in simulating tropical storm frequency, intensity, longitude, and latitude interannual variability over some of the ocean basins. Two variables may be highly correlated because both of them are dependent on the third variable. Therefore, linear correlations, and statistical tools in general, cannot prove a direct physical impact of one quantity on another, but they can demonstrate that there is no significant impact. As the linear correlations between the first EOF of SSTs calculated over each ocean basin and simulated tropical storm statistics are, in general, low and not significant, it can be concluded that local SSTs do not play a significant role in simulated tropical storm frequency, intensity, and location interannual variability, except maybe over the western North Pacific, south Indian Ocean, and South Pacific. The small role played by the local SSTs on tropical storm interannual variability is consistent with observations. The present paper focuses on the period 1980–88 where two strong El Niño events took place.

When the model is able to simulate an interannual variability of tropical storm frequency or location, this signal is strongly correlated with either the CEOF1 or CEOF2 time series of vertical wind shear, 850-mb vorticity, and 200-mb vorticity. The patterns of the CEOFs give a possible physical explanation for the strong correlations between the CEOF time series and the interannual variability of tropical storm parameters. This is a strong indication of a direct physical impact of the vertical wind shear, 850-mb vorticity, and 200-mb vorticity on tropical storm frequency or location.

The strong relationship between simulated tropical storms and simulated large-scale circulation cannot be explained by the impact of simulated tropical storms on the large-scale circulation, since over most of the basins the dominant mode in the large-scale circulation is ENSO related. Over some of the basins, such as the eastern North Pacific, the 200-mb vorticity seems to have the most significant impact on simulated tropical storm frequency. Over other basins, such as the south Indian Ocean, the 850-mb vorticity seems to explain the simulated tropical storm interannual variability, while over the South Pacific, tropical storms seem to be mostly constrained by the vertical wind shear. Therefore, each of the three fields (vertical wind shear, 850-mb vorticity, and 200-mb vorticity) has an important impact on simulated tropical storm frequency and location.

The ensemble displays skill in simulating the interannual variability of tropical storm frequency, longitude, and latitude over some basins. Over other basins, there are some major differences between simulated and observed tropical storm statistics. By comparing the observed and simulated large-scale circulation, the differences between observed and simulated tropical storm statistics can be explained by the lack of skill of the ensemble in simulating a realistic large-scale circulation. In other words, the significant anticorrelations between simulated and observed tropical storm frequency obtained over some basins such as the south Indian Ocean are probably not due primarily to a difference in physics between observed and simulated tropical storms, but rather to a difference in the large-scale circulation.

Several papers (McBride 1984; Evans 1992; Lighthill et al. 1994) have criticized the use of GCMs for tropical storm climatological studies, particularly for the study of global climate change. They assert that the coarse resolution of GCMs makes them an inappropriate tool for studies of these statistics. According to the results in the present study, the analogy between simulated and observed tropical storms seems to be good enough to be useful in some climatological studies. The fact that the large-scale circulation has a similar impact on simulated and observed tropical storms is an indication that the fundamental physical constraints on observed and simulated tropical storms may not be that different. The origin of simulated tropical storms is still an open question, but even if simulated tropical storm cyclogenesis is different from that observed, the sensitivity of simulated tropical storms to vertical wind shear, 850-mb vorticity, and 200-mb vorticity indicates that GCMs may be useful for the prediction of the interannual variability of tropical storm frequency and location.

Acknowledgments. The authors would like to thank R. Tuleya, Dr. N. Lau, and Dr. A. Broccoli for their stimulating discussions and help, and two anonymous

reviewers whose comments proved invaluable in improving the presentation of the material.

REFERENCES

Bengtsson, L., H. Böttger, and M. Kanamitsu, 1982: Simulation of hurricane-type vortices in a general circulation model. *Tellus*, **34,** 440–457.

——, M. Botzet, and M. Esh, 1995: Hurricane-type vortices in a general circulation model. *Tellus*, **47A,** 175–196.

Evans, J. L., 1992: Comment on ''Can existing climate models be used to study anthropogenic changes in tropical cyclone climate?'' *Geophys. Res. Lett.*, **19,** 1523–1524.

Frank, W. M., 1987: Tropical cyclone formation. *Global View of Tropical Cyclones*, R. L. Elsberry, Ed., Office of Naval Research, 53–90.

Gates, W., 1992: AMIP: The atmospheric model intercomparison project. *Bull. Amer. Meteor. Soc.*, **73,** 1962–1970.

Gordon, C. T., 1992: Comparison of 30-day integrations with and without cloud–radiation interaction. *Mon. Wea. Rev.*, **120,** 1244–1277.

——, and W. F. Stern, 1982: A description of the GFDL global spectral model. *Mon. Wea. Rev.*, **110,** 625–644.

Gray, W. M., 1968: Global view of the origin of tropical storm disturbances and storms. *Mon. Wea. Rev.*, **96,** 669–700.

——, 1979: Hurricanes: Their formation, structure and likely role in the tropical circulation. *Meteorology over the Tropical Oceans*, D. B. Shaw, Ed., Royal Meteorological Society, 155–218.

——, 1984: Atlantic seasonal hurricane frequency. Part I: El Niño and 30 mb quasi-biennial oscillation influences. *Mon. Wea. Rev.*, **112,** 1649–1668.

Kalnay, E., and Coauthors, 1996: The NCEP/NCAR 40-year reanalysis project. *Bull. Amer. Meteor. Soc.*, **77,** 437–471.

Knuth, D. E., 1981: *Seminumerical Algorithms*. Vol. 2, *The Art of Computer Programming*, Addison-Wesley, 688 pp.

Lighthill, J., G. Holland, W. Gray, C. Landsea, G. Graig, J. Evans, Y. Kurihara, and C. Guard, 1994: Global climate change and tropical cyclones. *Bull. Amer. Meteor. Soc.*, **75,** 2147–2157.

Manabe, S., 1969: Climate and the ocean circulation: I. The atmospheric circulation and the hydrology of the earth's surface. *Mon. Wea. Rev.*, **97,** 739–774.

——, J. Smagorinsky, and R. F. Strickler, 1965: Simulated climatology of a general circulation model with a hydrological cycle. *Mon. Wea. Rev.*, **93,** 769–798.

——, J. L. Holloway Jr., and H. M. Stone, 1970: Tropical circulation in a time-integration of a global model of the atmosphere. *J. Atmos. Sci.*, **27,** 580–613.

McBride, J. L., 1981a: Observational analysis of tropical cyclone formation. Part I: Basic description of data sets. *J. Atmos. Sci.*, **38,** 1117–1131.

——, 1981b: Observational analysis of tropical cyclone formation. Part III: Budget analysis. *J. Atmos Sci.*, **38,** 1152–1166.

——, 1984: Comments on ''Simulation of hurricane-type vortices in a general circulation model.'' *Tellus*, **36A,** 92–93.

——, and R. Zehr, 1981: Observational analysis of tropical cyclone formation. Part II: Comparison of non-developing versus developing systems. *J. Atmos. Sci.*, **38,** 1132–1151.

Press, W. R., 1986: *Numerical Recipes: The Art of Scientific Computing*. Cambridge University Press, 102 pp.

Sirutis, J., and K. Miyakoda, 1990: Subgrid scale physics in 1-month forecasts. Part I: Experiment with four parameterization packages. *Mon. Wea. Rev.*, **118,** 1043–1064.

Stern, W., and R. Pierrehumbert, 1988: The impact of orographic gravity wave drag parameterization on extended range predictions with a GCM. Preprints, *Eighth Conf. on Numerical Weather Prediction*, Baltimore, MD, Amer. Meteor. Soc., 745–750.

Tiedtke, M., 1988: Parameterization of cumulus convection in large-scale models. *Physically-Based Modeling and Simulation of Climate and Climate Change*, M. Schlesinger, Ed., D. Reidel, 375–431.

Tsutsui, J.-I., and A. Kasahara, 1996: Simulated tropical cyclones using the National Center for Atmospheric Research community climate model (1996). *J. Geophys. Res.*, **101,** 15 013–15 032.

Vitart, F., J. L. Anderson, and W. F. Stern, 1997: Simulation of interannual variability of tropical storm frequency in an ensemble of GCM integrations. *J. Climate*, **10,** 745–760.

Wu, G., and N.-C. Lau, 1992: A GCM simulation of the relationship between tropical-storm formation and ENSO. *Mon. Wea. Rev.*, **120,** 958–977.